

# **EVALUATION OF A NESTED VERSION OF THE WAVE MODEL WAM4.5 DURING THE DND'S FIELD EXPERIMENT NEAR HALIFAX, NOVA SCOTIA**

**Roop Lalbeharry**  
**Environment Canada, Science and Technology Branch**  
**Meteorological Research Division**  
**Toronto, Ontario, M3H 5T4**  
**Email : Roop.Lalbeharry@ec.gc.ca**

## **1. INTRODUCTION**

During the period 13-22 September 2005, the Department of National Defence (DND) conducted an exercise at Osborne Head about 20 km east of Halifax, Nova Scotia. The objective of the exercise was to assess the impact of the marine environment on its Shipboard Integration Sensors and Weapons Systems (SISWS) Technology Demonstration Program (TDP). The ship used was the CFAV Quest and the test area covered a 200 km x 200 km square centred on Osborne Head. The Canadian Meteorological Centre (CMC) agreed to provide nearshore shallow water wave forecasts of the sea state conditions which seem to have an important effect on the operations of some of the DND's weapons systems.

The chosen state-of-the-art model for this study is the open ocean wave model WAM Cycle-4.5 (hereinafter referred as WAM4.5). Earlier investigations with WAM Cycle-4.0 (hereafter referred as WAM4) applied to high resolution areas like coastal seas or lakes (e.g. Monbaliu et al. 2000, Liu et al. 2002, Soomere et al. 2005) demonstrated already that such an open ocean model performs practically as good as specific coastal wave models in terms of the basic wave parameters. The high resolution small-scale version of WAM4 that has been introduced by Monbaliu et al. (2000) includes several numerical adjustments related to small spatial scales. These improvements are included also in the new standard version WAM4.5 except the choices of using an octant or quadrant coordinate system for the propagation of the wave energy and time-dependent current field. The WAM4.5 was run with three different grid resolutions producing wave forecasts up to 48 hours twice daily at 0000 UTC and 1200 UTC, respectively, for the month of September 2005 which includes the DND's exercise period. The model results obtained for each of the three grid resolutions are compared with available observations at three buoy locations located inside the exercise area.

The primary objective of this study is to assess the performance of the WAM4.5 at various grid resolutions. The modelling description is briefly described in section 2. Section 3 discusses the buoys used for validation. Discussions about the wave model results in comparison with buoy measurements and a corresponding statistical analysis are presented in section 4, followed by summary and conclusions in section 5.

## **2. MODELLING DESCRIPTION**

### **2.1 THE WAM4.5**

The WAM (**WA**ve **M**odel) is originally developed for open ocean applications and provides reliable data on a global or regional scale down to model grid sizes about two kilometres and water depths above about 5 m. It solves the energy balance equation for

no currents and fixed water depths on a spherical grid and in frequency-direction space. The physics of the model are contained in the net source term expressed in terms of energy density  $E(f, \theta, \phi, \lambda, t)$ , where  $f$  is frequency,  $\theta$  wave direction,  $\phi$  latitude,  $\lambda$  longitude, and  $t$  time. It is the sum of a number of source terms representing the effects of wave generation by wind (linear growth and exponential growth), quadruplet nonlinear wave-wave interactions, dissipation due to whitecapping, bottom friction and depth-induced wave breaking. The quadruplet nonlinear wave-wave interaction source term transfers energy from spectral peaks to lower and higher frequencies. The energy is redistributed so that there is no net loss or gain of energy due to nonlinear wave-wave interactions. This source term dominates the evolution of the spectrum in deep and intermediate waters and is computed with the discrete interaction approximation method of Hasselmann et al. (1985).

WAMDI Group (1988) describes the Cycle-3 version of the WAM (hereafter referred as WAM3) in which the exponential wind input and whitecapping source terms are based on the formulations of Komen et al. (1984). In the WAM4 version the corresponding source terms are based on the formulations of Janssen (1989, 1991) in which the winds and waves are coupled so that there is a feedback of growing waves on the wind profile. The effect of this feedback is to enhance the wave growth of younger wind seas over that of older wind seas for the same wind. The WAM4.5 is an update of the WAM4 and incorporates many of the changes described in Monbaliu et al. (2000). It uses the first order upwind explicit propagation scheme which results in the propagation time step being limited by the CFL condition and a fully implicit source term integration scheme. The latter enhancement allows the specification of the source term integration time step to be larger than the propagation time step. To ensure that the WAM remains numerically stable a limitation on wave growth is imposed. This limiter is based on the formulation of Hersbach and Janssen (1999) and gives the maximum total change of energy density per iteration per spectral wave component. The Phillip's linear growth term is added to the WAM4.5 as it was excluded in earlier versions of the WAM. This source term is based on the formulation of Cavaleri and Malanotte-Rizzoli (1981) and allows wave growth at low wind speeds. The bottom friction source term is based on the empirical JONSWAP model of Hasselmann et al. (1973) in which the dissipation constant is a tuning parameter set to  $0.038 \text{ m}^2\text{s}^{-3}$  in this study. The dissipation source term due to depth induced wave breaking is included but not activated in this study. More details of the formulation of the WAM can be found in Komen et al. (1994).

## 2.1 MODEL SETUP

The wave model set up includes a coarse grid WAM4.5 (denoted as WAM-CG) with a resolution of  $0.5^\circ$  covering the area  $25\text{N} - 70.0\text{N}/82.0\text{W} - 0\text{W}$ , a fine grid WAM4.5 (denoted as WAM-FG) with a resolution of  $0.1^\circ$  nested inside the coarse grid and covering the area  $40.0\text{N} - 52.0\text{N}/74.5\text{W} - 46.0\text{W}$  and an extra fine grid WAM4.5 (denoted as WAM-XFG) with a resolution of  $0.05^\circ$  nested within the fine grid and covering the area  $42.5\text{N} - 45.5\text{N}/66.0\text{W} - 61.5\text{W}$ . The areas covered by the three grids are shown in Fig. 1. The coarse grid WAM4.5 provides the spectral boundary conditions for the fine grid WAM4.5 which, in turn, provides the boundary conditions for the extra fine grid. The assumption of no currents implies that changes to the mean wave direction are due only to depth refraction. In order to assess its impact the extra fine grid WAM4.5 is run with and without depth refraction. The solution of the energy balance equation is

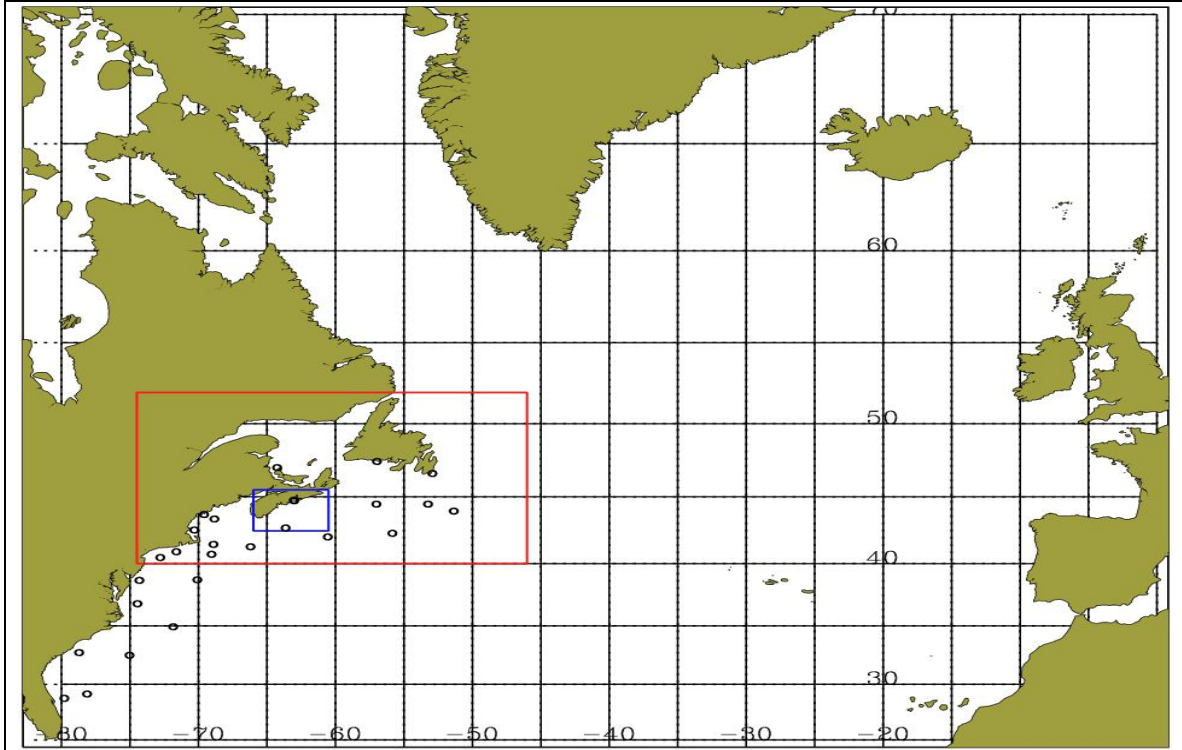


Fig. 1: Wave model areas covered by the three grid resolutions used in this study, namely, a coarse grid in black outline with grid resolution of  $0.5^\circ$ , a fine grid in red outline with grid resolution of  $0.1^\circ$ , and an extra fine grid in blue outline with grid resolution of  $0.05^\circ$ .

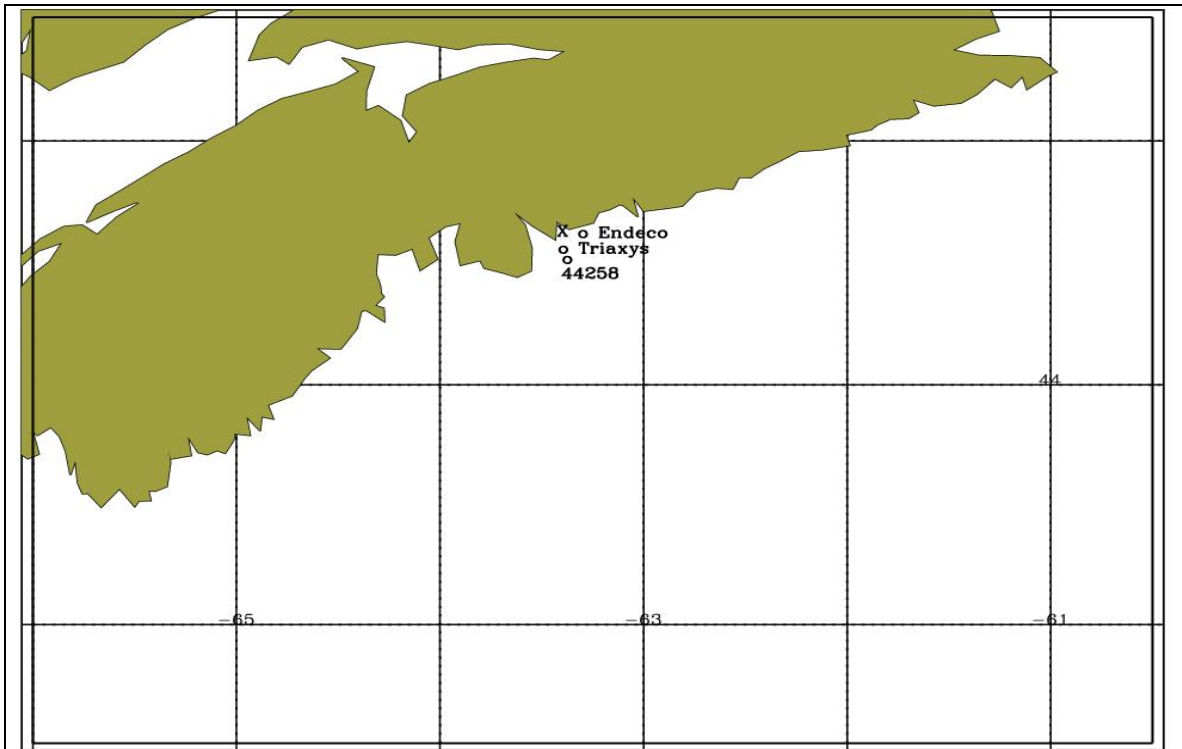


Fig. 2: Enlarged extra fine grid area given in Fig. 1 showing the locations of the three validation buoys used in this study. The “X” denotes the location of Osborne Head.

provided for 25 frequencies logarithmically spaced from 0.042 Hz to 0.41 Hz at intervals of  $\delta f/f = 0.1$  and 24 directional bands at  $15^\circ$  each with the first direction being  $7.5^\circ$  measured clockwise with respect to true north. The three versions of the WAM4.5 are run in shallow water mode twice daily at 0000 UTC and 1200 UTC, respectively, producing wave forecasts up to 48 hours for the month of September 2005 which includes the DND's experiment period of 13-22 September. The WAM-XFG run wave forecasts giving the sea state conditions were made available to the CFAV Quest for use in assessing their impact on DND's weapons systems. Since the wave model runs in a forecast mode, a quasi-hindcast wave dataset for the period of this study for analysis is created by assembling the 0, 1, 2, ....., and 11 forecast outputs of the 0000 and 1200 UTC wave model daily runs.

## 2.2 MODEL INPUTS

The primary inputs to the WAM4.5 are the bathymetry, the wind forcing and the ice field. The bathymetry for each grid varies from a minimum of 5 m to a maximum of 999 m. Water depths less than 5 m are set to 5 m and those greater than 999 m to 999 m. Each model run is forced by the 10 m level surface winds obtained from the CMC regional GEM (Global Environmental Multiscale) weather prediction model at three-hourly intervals for a forecast period up to 48 hours. The winds are first generated on the GEM model grid and then interpolated onto the wave model three grids. The ice field is obtained from the CMC sea ice analysis at the beginning of each model run and remains unchanged throughout the forecast period. The model grid point is considered to be a sea point if the ice fraction at that point  $> 0.5$ . At all land points, and at all sea ice points, the wave energy of each spectral component is set equal to zero. It should be noted that the areas covered by the fine and extra fine grids were generally ice-free during the period of this study.

## 3. VALIDATION BUOYS

The validation buoys include one buoy from the Canadian buoy network and two extra wave directional wave buoys deployed by DND for the SISWS experiment, namely, buoy ENDECO at location 44.6058N/63.3223W and buoy TRIAXYS at 44.5417N/63.4200W as shown in Fig. 2. The Halifax Harbour buoy 44258 at 44.50N/63.40N and the buoys ENDECO and TRIAXYS all lie inside the extra fine grid area. The outputs from the WAM4.5 at the three grid resolutions are validated against the available observations from the moored buoy 44258 and against the two DND's buoys. Data from buoy 44258 are available for the entire month of September, from the buoy Endeco for the period 13-22 September and from the buoy Triaxys for the period 13-18 September. The validation datasets were obtained from the Marine Environmental Data Service (MEDS) in Canada for buoy 44258 and from DND for the buoys Endeco and Triaxys. The wind/wave parameters include significant wave height (SWH or  $H_s$ ), wave peak ( $T_p$ ) period and one dimensional (1-d) spectral energy density from all three buoys, mean wave period and mean wave direction from the buoys Endeco and Triaxys, and winds from buoys 44258 and Endeco. The wave data from the buoy Triaxys are based on the maximum entropy method (MEM) while those from the buoy Endeco are based on the average of MEM and the digital bandpass filtering method.

## 4. RESULTS AND DISCUSSIONS

Time series of model results obtained using the three grid resolutions and compared against available observations are presented for significant wave height (SWH or  $H_s$ ), peak period ( $T_p$ ), and one-dimensional (1-d) wave spectra for buoys 44258, Endeco and Triaxys, mean period ( $T_m$ )

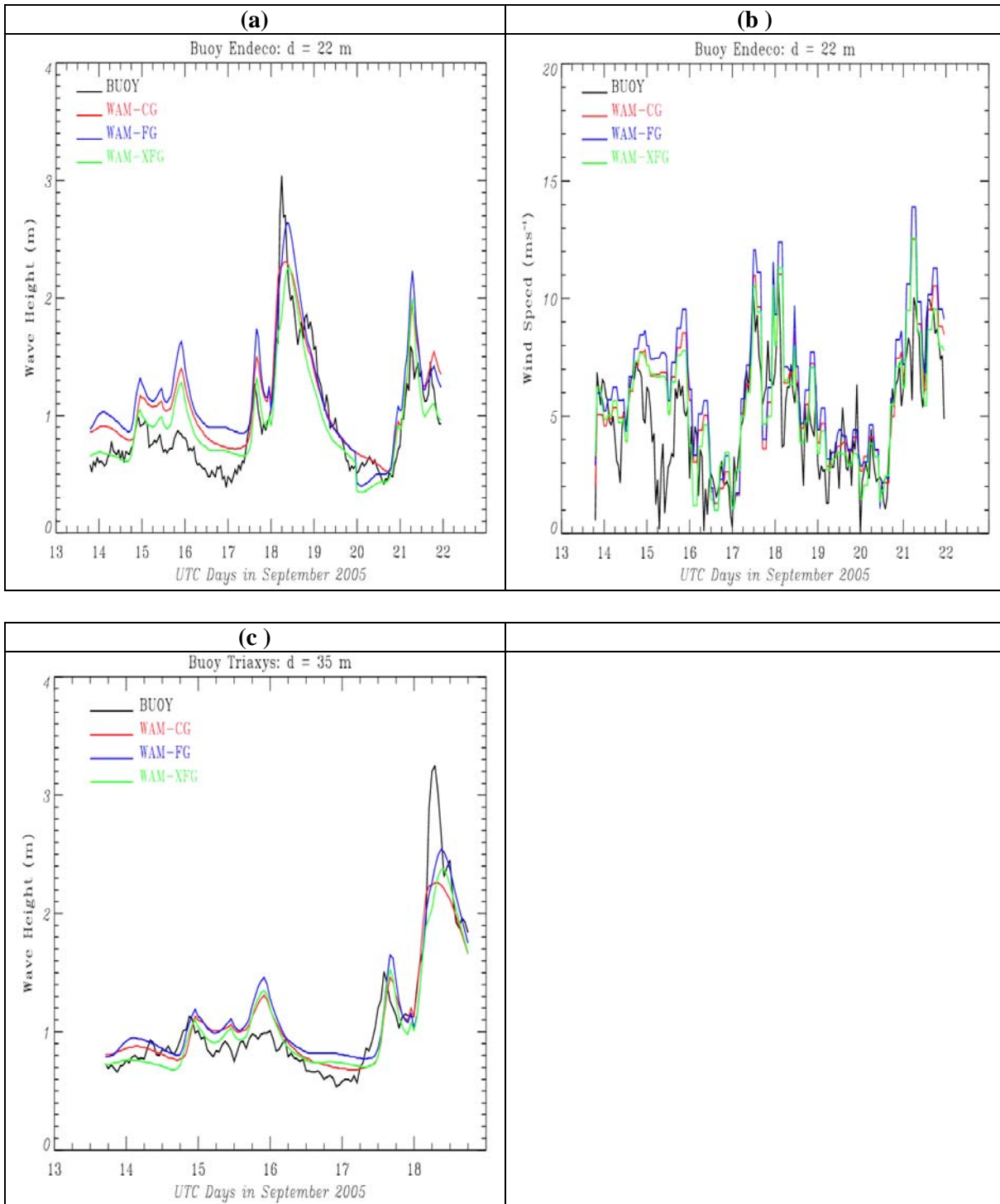


Fig. 3: Time series of significant wave height (SWH or  $H_s$ ) and wind speed. (a) gives the SWH and (b) the wind speed for buoy Endeco while (c) gives the SWH for buoy Triaxys for the period of available observations. In the figure legend CG denotes coarse grid run, FG fine grid run and XFG extra fine grid run.

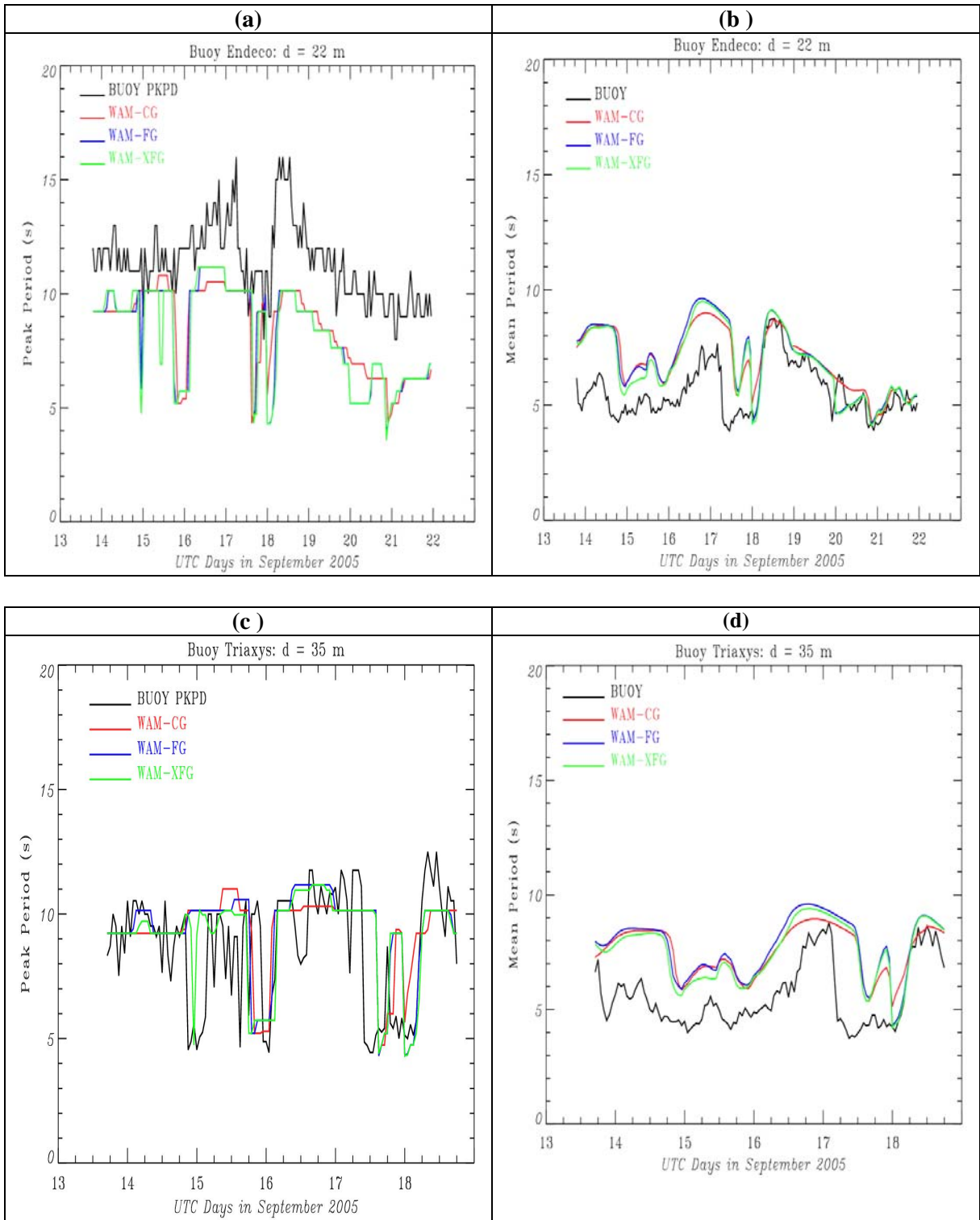


Fig. 4. Same as Fig. 3 but for peak and mean periods. (a) gives the peak period and (b) the mean period for buoy Endeco while (c) and (d) give the corresponding periods for buoy Triaxys.

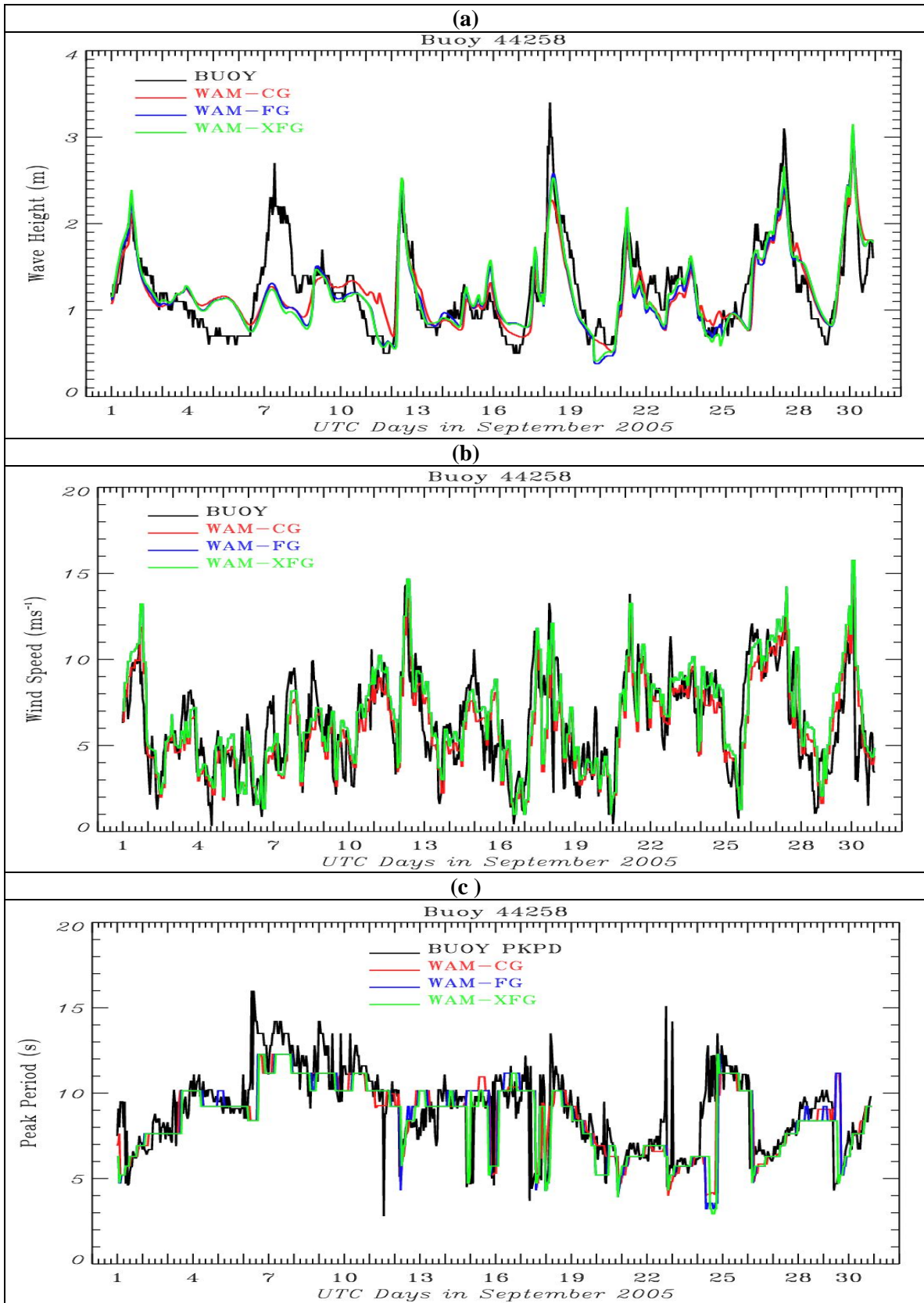


Fig. 5: Same as Fig. 3 but for buoy 44258 and for the entire month of September 2005.

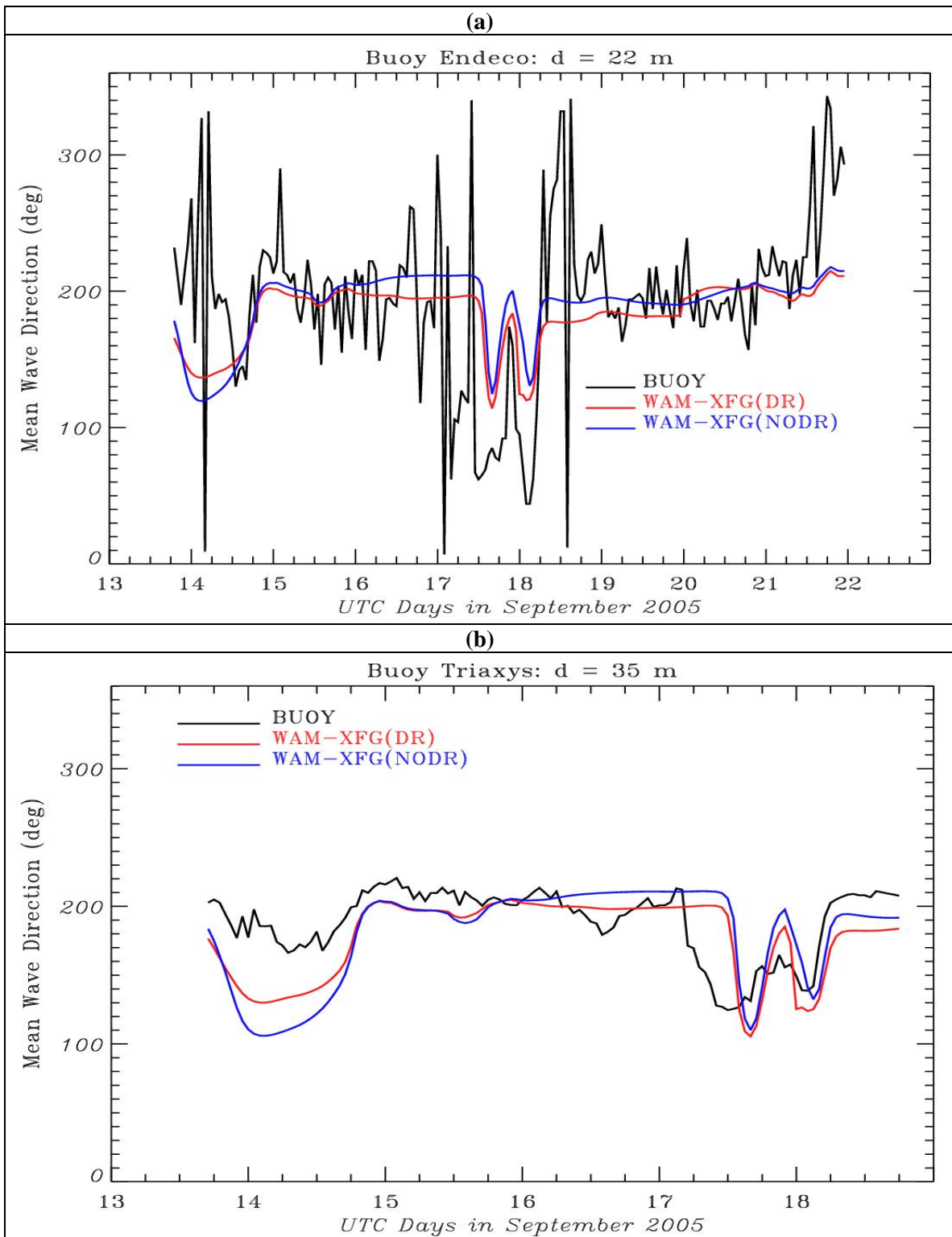


Fig. 6: Time series of mean wave direction for (a) buoy Endeco for the period 13-21 September and (b) buoy Triaxys for the period 13-18 September. In the figure legend XFG(DR) denotes extra fine grid run with depth refraction and XFG(NODR) that without depth refraction .

for buoys Endeco and Triaxys, and 10-m level wind speed ( $U_{10}$ ) for buoys 44258 and Endeco. The mean wave direction ( $\theta_m$ ) is presented for buoys Endeco and Triaxys and is restricted to the extra fine grid version of the WAM4.5 since only the latter is run with and without depth refraction.

The model and observed SWH and  $U_{10}$  for the buoy Endeco are shown, respectively, in Fig. 3a and Fig. 3b while the corresponding SWH for the buoy Triaxys is presented in Fig. 3c. It is seen that during the DND's experiment period, there is only one major wave episode with a maximum  $H_s$  of 3 m occurring around 0600 UTC 18 September. The model does not only underpredict this peak but its occurrence lags the observed peak by 1-3 hours for the three different grid runs. This occurs at both buoys Endeco and Triaxys. However, the WAM-FG run does a somewhat better job than both the WAM-CG and WAM-XFG runs in generating the peak SWH. The model wind speed shown in Fig. 3b is generally overpredicted. Since the anemometer is at a height of 1.5 m on the buoy Endeco, the adjustment of the wind speed based on neutral stability to the 10 m level seems to suggest that the correction factor may be somewhat small.

The peak and mean periods for the buoy Endeco are shown, respectively, in Fig. 4a and Fig. 4b and the corresponding ones for the buoy Triaxys in Fig. 4c and Fig. 4d. The observed  $T_p$  shows more spikiness while that of the model is more stepwise. For the buoy Endeco the three model runs underpredict the  $T_p$  throughout the period of the exercise. However, for both buoys the model peak periods are more consistent in their behaviour when compared with one another. The mean period  $T_m$ , however, is overpredicted but follows closely the behaviour of the observed  $T_m$  for both buoys. When comparing the peak periods of the three model runs, differences among the periods are, at most, minimal with hardly any difference between those of the WAM-FG and WAM-XFG runs. The same is also true for the mean period  $T_m$ .

Model outputs are compared against the observations of buoy 44258 in Fig. 5 for the month of September. In Fig. 5a there are six SWH peaks ranging from 2.4 m to 3.4 m, three of which are underpredicted and the other three overpredicted. The major peak of 3.4 m at 0600 UTC 18 September is underpredicted by the three model runs by 0.9 m to 1.2 m which is also true in the case of the other two buoys. Although the model SWH peaks are somewhat overestimated or underestimated, their times of occurrence are in fairly good agreement with those of the observed SWH peaks. This reflects the good agreement also between the timings of the model and buoy wind speed peaks as shown in Fig. 5b. It should be noted that the WAM-FG SWH is almost identical to the WAM-XFG SWH, suggesting that the WAM-FG, instead of the WAM-XFG, can be used for nearshore applications with some measure of confidence. The peak periods for the three model runs in Fig. 5c are consistent with one another and seem to follow reasonably well the behaviour of the observed  $T_p$ . However, the agreement between the model and buoy  $T_p$  shown in Fig. 4 is somewhat poorer. This seems to suggest that the method used for computing the peak period of the two DND buoys probably needs further examination.

The extra fine WAM4.5 is run with and without depth refraction to assess the impact of the water depth on the mean wave direction  $\theta_m$ . The results of the two WAM-XFG runs are compared with the  $\theta_m$  measurements made by buoys Endeco and Triaxys and are given in Fig. 6. It can be seen that the  $\theta_m$  in Fig. 6a made by the buoy Endeco shows more variations than the  $\theta_m$  in Fig. 6b made by the buoy Triaxys. The model  $\theta_m$  shows better agreement with that of the buoy Triaxys. Given the proximity of the two buoys and that the model  $\theta_m$  is quite similar at both buoy locations, the buoy Triaxys  $\theta_m$  appears to be more acceptable.

The time evolution of the observed 1-d spectra ( $m^2Hz^{-1}$ ) contoured in terms of colored scales at hourly intervals valid 18 September for a 24-hour period is shown for the buoys Endeco in Fig.

7a, Triaxys in Fig. 7b and 44258 in Fig. 7c. The main wave episode common to all three buoys occur during this period. The main observed spectral peak in each of the three buoys occurs around 0600 UTC 18 September and agrees reasonably well with the time of occurrence of the SWH peak shown for the corresponding buoys in Figs. 3 and 5. The observed peak frequency  $f_p$  obtained from the spectral measurements is near 0.09 Hz, that is, a  $T_p$  of 11 s. At 0600 UTC 18 September the Triaxys and 44258 peak periods are in good agreement with this value but the buoy Endeco gives a somewhat large value of 15 s. Because of the close similarity of the 1-d spectra of the three buoys, the spectra for the three model runs for the same period are compared against the buoy 44258 spectra and the results are presented in Fig. 8. The model spectra are 24-hour forecast spectra at hourly intervals based on the 0000 UTC 18 September model run. The three model runs each gives a  $T_p$  of 10 s with the observed being 11 s. The first appearance of the peak spectral intensity occurs at 0900 UTC 18 September, some 3 hours later than the observed peak spectral intensity. The WAM-CG run produces weaker intensity while the intensities of the WAM-FG and WAM-XFG runs are quite similar.

Snapshots of the SWH outputs valid 0800 UTC 18 September based on the three different grid resolutions are displayed mainly for the extra fine grid area in Fig. 9. The contour patterns from these runs all look similar. However, the WAM-FG and WAM-XFG 2.5 m contours are closer to the coastal areas than that of the WAM-CG. This highlights the importance to wave forecasters in running a finer grid resolution model, possibly in a nested mode, to better delineate areas of maximum SWH near the coasts.

Fig. 10 presents scatter plots of model versus observed wave heights available from the three buoys used in this study for September 2005. The solid black lines denote perfect fit to model and observed values and the blue lines the best fit linear regression lines with slopes  $b$  and  $y$ -intercepts. The plots complement the model statistics in Table 1 discussed below and they provide a more appealing way of displaying the same information. The plots indicate that the three grid resolutions used produced results that are quite similar when compared with the observations. For SWH the scatter is about the same in all three grid runs.

The buoy data provide an independent data set to objectively evaluate the accuracy or quality of the model wave parameters. Table 1 presents the validation statistics for both the significant wave heights and peak periods for the three model runs. In the Table the coarse grid run statistics are denoted as WAMC, the fine grid run as WAMF and the extra fine grid run as WAMXF. A positive bias denotes overprediction and a negative bias underprediction by the model. In the computations of the anomaly correlation,  $ac$ , and the reduction of variance,  $rv$ , the buoy mean of all the observations is used as climatology. The parameters  $ac$  and  $rv$  are skill scores since they provide a measure of how much more skill the model wave parameter has over the unskilled estimate based on climatology. The model value is considered to be useful if the  $ac$  exceeds the threshold value of 0.6 or 60% (Janssen, 1997) and better than climatology for  $rv > 0.0$ . An examination of the SWH statistics indicates that the performances of the three versions of the WAM4.5 are about the same. For the SWH simulation the models show some skill in the sense that the  $ac > 60\%$  and the  $rv$  is close to 0.7 and positive. The statistics for  $T_p$  show less skill with  $ac < 60\%$  and  $rv < 0.13$ . The scatter index  $SI$  ( $= rmse/buoy\ mean$ ), another skill index, is about 25% for both the SWH and  $T_p$ . The objective is to achieve a  $SI$  of the order of 15%. The differences between the WAMC and WAMF statistics and between the WAMF and WAMXF statistics are rather minimal. In other words, in deep and intermediate water depths the performance of the coarse grid WAM4.5 is quite comparable with those of the nested fine and extra fine grid versions of the WAM4.5. The implication of this is that the WAM-CG version may be adequate to produce regional operational wave forecasts in the areas of interest of the Canadian wave forecasting centres but for nearshore applications the WAM-FG, rather than the

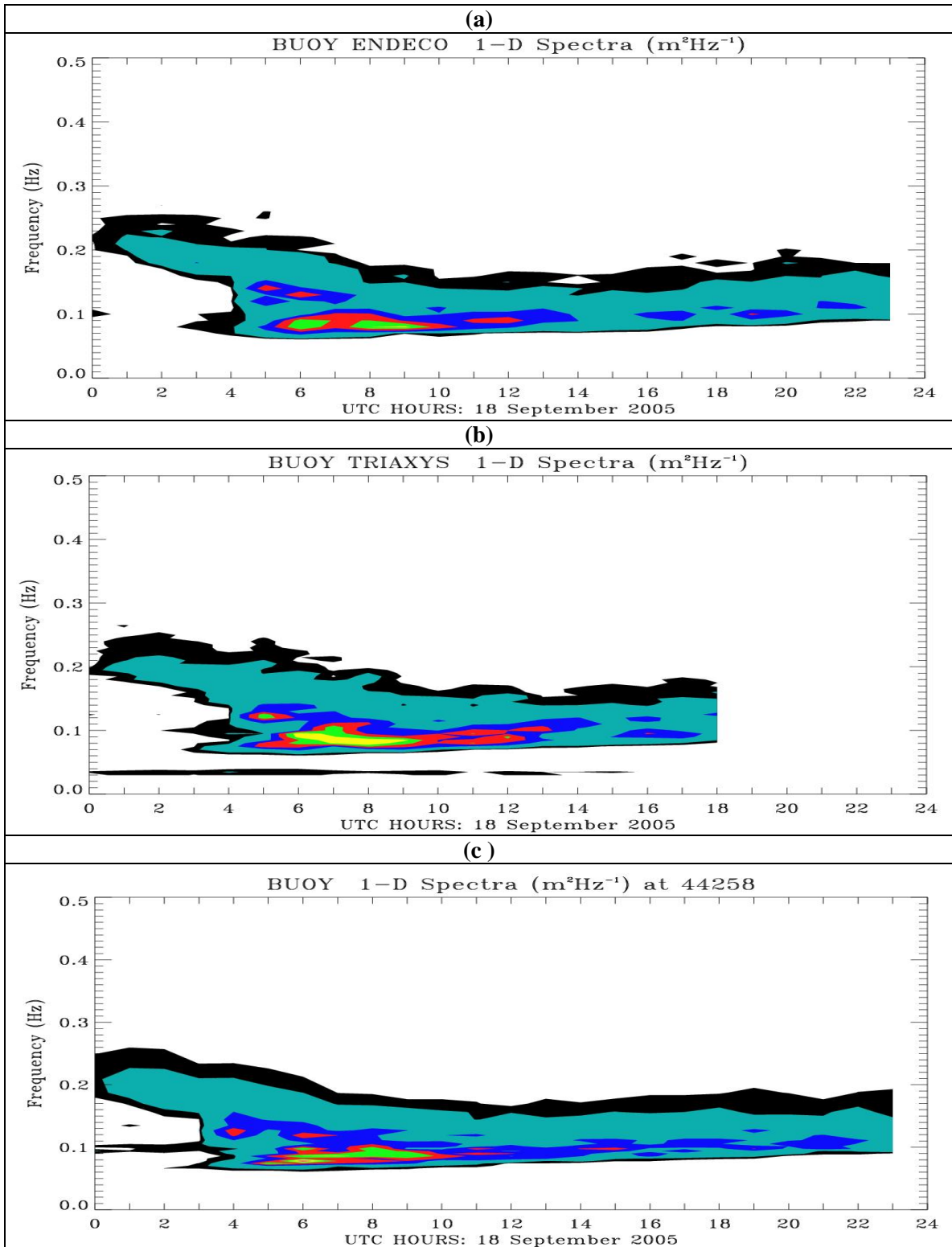


Fig. 7: Time evolution of observed 1-d spectra at hourly intervals valid 18 September 2005 for a 24-hour period at the locations of buoys (a) Endeco, (b) Triaxys and (c ) 44258. The coloured areas are energy density levels in  $\text{m}^2\text{Hz}^{-1}$ , namely, black (0.5-1), turquoise (1-4), blue (4-7), red (7-10), green(10-13) and yellow (13-16).

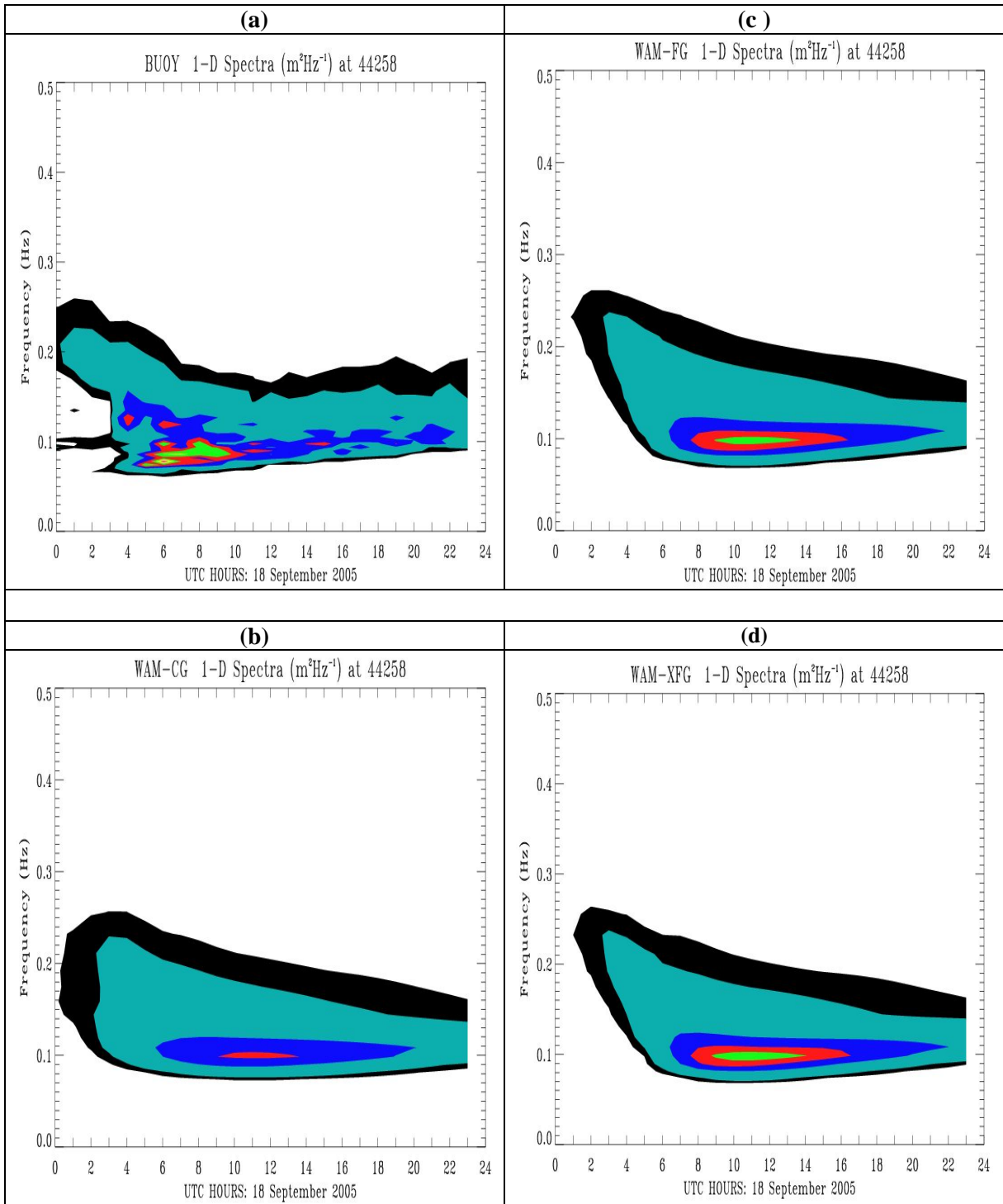


Fig. 8: The forecast 1-d spectra at hourly intervals for a 24-hour period, obtained from the 0000 UTC model runs valid 18 September 2005, are compared against the buoy 44258 1-d spectra for the same period. The spectra shown are (a) buoy 44258, (b) the WAM-CG run, (c) the WAM-FG and (d) the WAM-XFG run. The coloured areas are energy density levels in  $\text{m}^2\text{Hz}^{-1}$ , namely, black (0.5-1), turquoise (1-4), blue (4-7), red (7-10), green (10-13) and yellow (13-16).

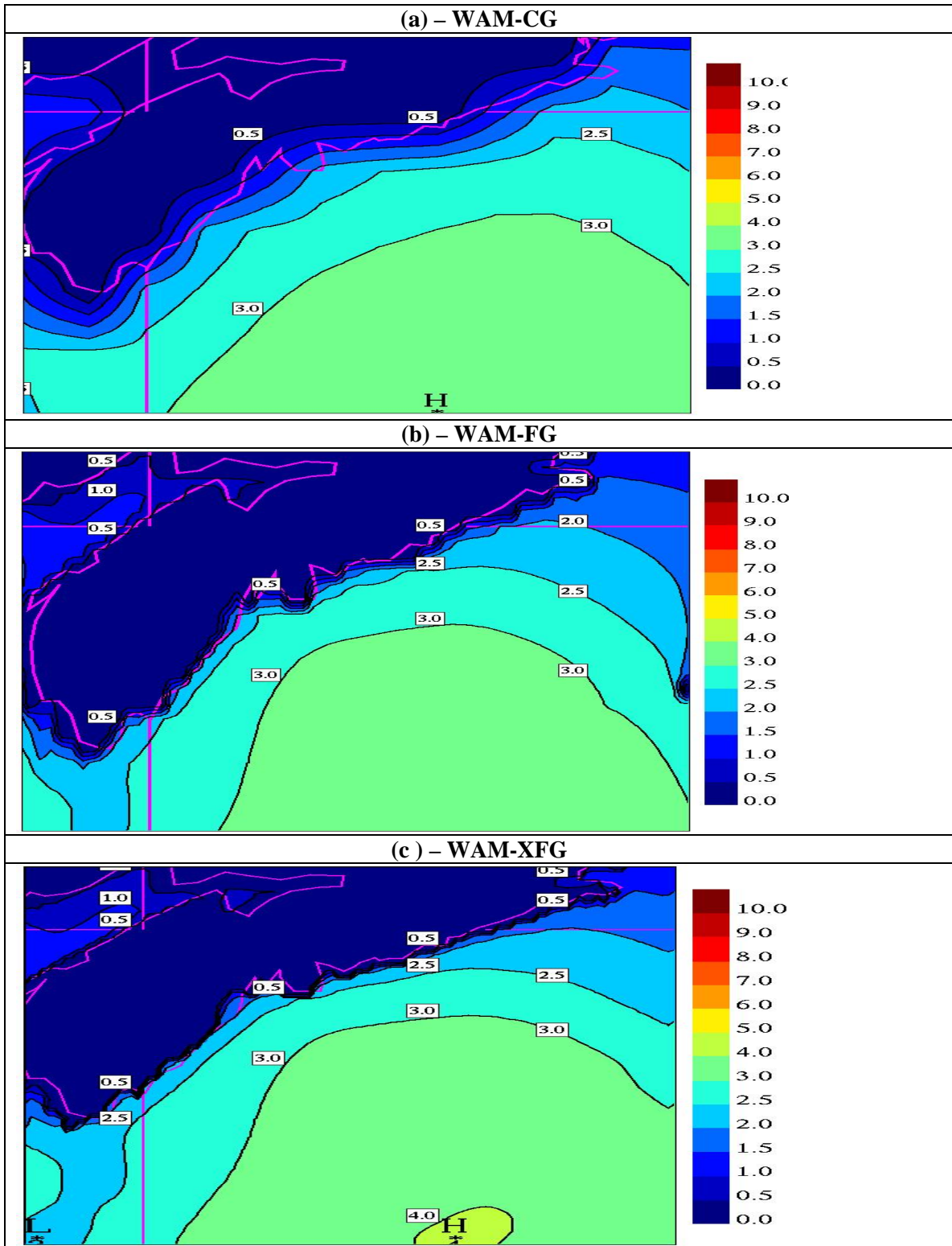


Fig. 9: Snapshots of model SWH (m) valid 0800 UTC 18 September 2005 for (a) the WAM-CG run, (b) the WAM-FG run and (c) the WAM-XFG run. The model outputs from the three different grid resolution runs are displayed mainly for the extra fine grid area.

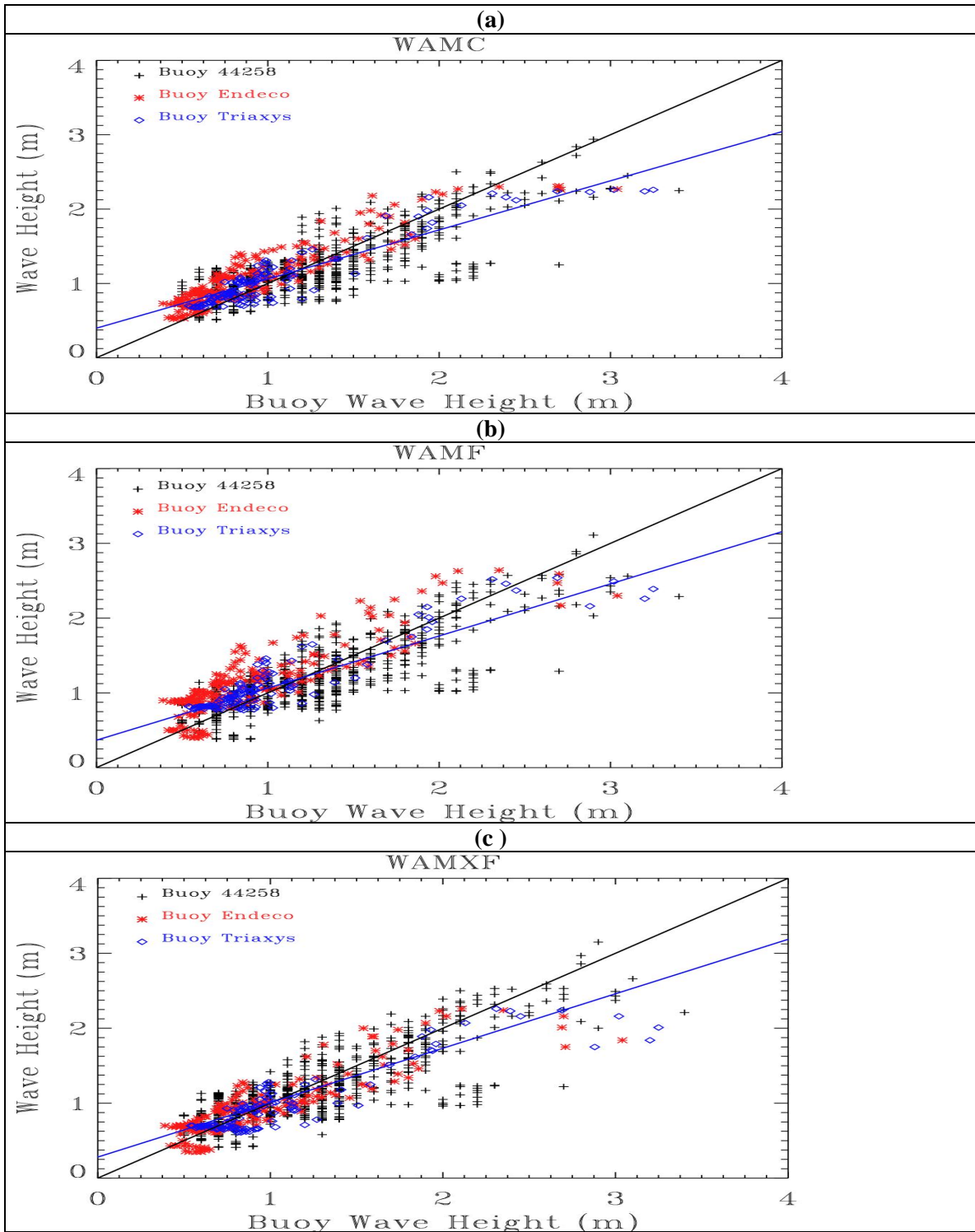


Fig. 10: Scatter plots of model versus observed SWH (m) based on the available observations from the three buoys Endeeco, Triaxys and 44258 located in the extra fine grid area for September 2005. In the figure WAMC denotes the coarse grid run shown in (a), WAMF the fine grid run in (b) and WAMXF the extra fine grid run in (c). The black lines denote the perfect fit to model and observed values and the blue lines the best fit linear regression lines.

**Table 1:** Validation statistics for significant wave heights  $\geq 0.1$  m and peak period  $\geq 2.0$  s based on the observations available for September 2005 for the different wave model runs (SI: Scatter index, r: linear correlation coefficient, ac: anomaly correlation, rv: reduction of variance, a: intercept and b: slope of the linear regression line and N: number of observations). WAMC, WAMF and WAMXF are as defined in Fig. 10.

	<b>WAVE HEIGHT STATISTICS (m)</b>		
	<b>WAMC</b>	<b>WAMF</b>	<b>WAMXF</b>
Buoy mean	1.166	1.166	1.166
Model mean	1.169	1.180	1.127
Bias	0.003	0.014	-0.039
Rmse	0.289	0.302	0.289
SI	0.248	0.259	0.248
r	0.836	0.820	0.840
ac	0.837	0.821	0.837
rv	0.697	0.671	0.699
a	0.399	0.367	0.281
b	0.661	0.697	0.726
N (no. of obs.)	1039	1039	1039
	<b>PEAK PERIOD STATISTICS (s)</b>		
	<b>WAMC</b>	<b>WAMF</b>	<b>WAMXF</b>
Buoy mean	9.424	9.424	9.424
Model mean	8.703	8.645	8.505
Bias	-0.721	-0.779	-0.919
Rmse	2.264	2.382	2.329
SI	0.240	0.253	0.247
r	0.535	0.511	0.555
ac	0.502	0.479	0.508
rv	0.128	0.036	0.078
a	4.671	4.500	4.054
b	0.428	0.440	0.472
N (no. of obs.)	1039	1039	1039

WAM-XFG, can be nested inside the WAM-CG, thus saving valuable computer time. This is demonstrated also in Fig. 9b with regards to the representation of wave height contours near the coast.

## 5. SUMMARY AND CONCLUSIONS

In this study three versions of the WAM4.5, namely, a coarse grid, a fine grid nested inside the coarse grid and an extra fine grid nested inside the fine grid are utilized in numerical wave simulations during the DND's SISWS field experiment of September 2005 at Osborne Head about 20 km east of Halifax. The main objective of this study is to assess the performance

of the WAM4.5 at various grid resolutions. The model results are validated against three buoys located in close vicinity of one another and inside the exercise area as shown in Fig. 2. Two of the buoys, Endeco and Triaxys, are deployed by DND during the exercise period of 13-22 September while the third buoy 44258 belongs to the Canadian buoy network which made observations for the entire month of September.

The three versions of the WAM4.5 produce results that are in close agreement with one another. However, the fine and extra fine grid versions give a better representation of the nearshore wave height contours. All three model runs underpredict the major observed peak SWH of 3 m common to the three buoys at 0600 UTC 18 September and show that the times of occurrence of this peak vary from 1-3 hours. The model winds are reasonably accurate when compared with buoy 44258 winds. However, when compared with the buoy Endeco winds, the model winds are overestimated which may be due to the correction factor based on neutral stability used in adjusting the observed winds from the anemometer level of 1.5 m to the 10 m level being somewhat small. The peak periods from the three model runs show a stepwise behaviour. They are generally consistent with one another and are not well simulated when compared with the observed peak period because of the spiky nature of the latter. However, the forecast peak periods calculated from the 1-d spectra produced by the three model runs are closer to the observed value derived from the buoy 44258 1-d spectra valid 0600 UTC 18 September but they all occur some 3 hours later than the observed. The corresponding model mean periods are also consistent with one another and in better agreement with the observed mean period. In this study the WAM-XFG is run with and without depth refraction and the results indicate that activation of depth refraction does not have a significant impact on the mean wave direction when compared with the observations. The model wave statistics for SWH and  $T_p$  show minimal differences. This seems to suggest that the WAM-CG version may be adequate to produce regional operational wave forecasts for deep and intermediate waters but for nearshore applications the nested version WAM-FG, rather than the nested version WAM-XFG, can be used with some measure of confidence.

## REFERENCES

- Cavaleri, L. and P. Malanotte-Rizzoli, 1981: Wind wave prediction in shallow water: Theory and applications. *J. Geophys. Res.*, 86, 10961-10973.
- Hasselmann, K., T. P. Barnett, K. Bouws, H. Carlson, D. E. Cartwright, K. Enke, J. I. Ewing, H. Gienapp, D. E. Hasselmann, P. Kruseman, A. Meerburg, P. Muller, K. Richter, D. J. Olbers, W. Sell and H. Walden, 1973: Measurements of wind-wave growth and swell decay during the Joint North Sea Wave Project (JONSWAP), *Dtsch. Hydrogr. Z. Suppl.*, 12, A8, 95p.
- Hasselmann, K., D. B. Ross, P. Müller, W. Sell, 1976: A parametrical wave prediction model. *J. Phys. Oceanogr.*, 6, 201-228.
- Hasselmann, S., K. Hasselmann, J. H. Allender and T. P. Barnett, 1985: Computations and parameterizations of the nonlinear energy transfer in a gravity-wave spectrum. Part II: Parameterizations of the nonlinear transfer for application in wave models. *J. Phys. Oceanogr.*, 19, 745-754.
- Hersbach, H. and P. A. E. M. Janssen, 1999: Improvement of the short-term behaviour in the wave ocean model (WAM). *J. Atmos. Oceanic Techn.*, 16, 884-892.

- Janssen, P. A. E. M., B. Hansen, and J. R. Bidlot, 1997: Verification of the ECMWF wave forecasting system against buoy and altimeter data. *Wea. Forecasting*, 12, 763-784.
- Janssen, P. A. E. M. (1989) Wave-induced stress and the drag of air flow over sea waves *J. Phys. Oceanogr.*, 19, 745-754.
- Janssen, P. A. E. M., 1991: Quasi-linear theory of wind-wave generation applied to wave forecasting. *J. Phys. Oceanogr.*, 21, 1631-1642.
- Komen, G. J., L. Cavaleri, M. Donelan, K. Hasselmann, S. Hasselmann, and P. A. E. M. Janssen, 1994: *Dynamics and Modelling of Ocean Waves*, Cambridge University Press, Cambridge, 532p.
- Komen, G. J., S. Hasselmann and K. Hasselmann, 1984: On the existence of a fully developed windsea spectrum. *J. Phys. Oceanogr.*, 14, 1271-1285.
- Liu, Paul C., David J. Schwab and Robert E. Jensen, 2002: Has wind-wave modeling reached its limit? *Ocean Eng.*, 29, 81-98.
- Monbaliu, Jaak, Roberto Padilla-Hernandez, Julia C. Hargreaves, Juan Carlos Albiach, Weimin Luo, Mauro Sclavo and Heinz Guenther, 2000: The spectral wave model, WAM, adapted for applications with high resolution. *Coastal Eng.*, 41, 41-62
- Soomere, Tarmo, 2005: Wind wave statistics in Tallinn Bay: *Boreal Environmental Research*, 10, 103-118.
- WAMDI Group, 1988: The WAM model - A third generation ocean wave prediction model. *J. Phys. Oceanogr.*, 18, 1775-1810.